doi:10.1016/j.jmb.2010.11.053 J. Mol. Biol. (2011) xx, xxx–xxx

Contents lists available at www.sciencedirect.com

Journal of Molecular Biology

journal homepage: http://ees.elsevier.com.jmb

Nucleotide Pocket Thermodynamics Measured by EPR Reveal How Energy Partitioning Relates Myosin Speed to Efficiency

Thomas J. Purcell[1,2]*, Nariman Naber[1], Kathy Franks-Skiba[1,2], Alexander R. Dunn[3], Catherine C. Eldred[4], Christopher L. Berger[5], András Málnási-Csizmadia[6], James A. Spudich[7], Douglas M. Swank[4], Edward Pate[8] and Roger Cooke[1,2]

[1]*Department of Biochemistry and Biophysics, UCSF MC 2240, Genentech Hall Room S416C, 600 16th Street, San Francisco, CA 94158-2517, USA*
[2]*Cardiovascular Research Institute, University of California, San Francisco, CA 94158, USA*
[3]*Department of Chemical Engineering, Stanford University, Stanford, CA 94305, USA*
[4]*Department of Biology, Rensselaer Polytechnic Institute, Troy, NY 12180, USA*
[5]*Department of Molecular Physiology and Biophysics, College of Medicine, University of Vermont, Burlington, VT 05405, USA*
[6]*Department of Biochemistry, Eötvös Lorand University, Budapest 1117, Hungary*
[7]*Department of Biochemistry, Stanford University School of Medicine, Stanford, CA 94305, USA*
[8]*Department of Mathematics, Washington State University, Pullman, WA 99164, USA*

Received 1 July 2010; received in revised form 24 November 2010; accepted 26 November 2010

Edited by M. Moody

Keywords:
myosin;
actin;
muscle;
efficiency;
EPR spectroscopy

We have used spin-labeled ADP to investigate the dynamics of the nucleotide-binding pocket in a series of myosins, which have a range of velocities. Electron paramagnetic resonance spectroscopy reveals that the pocket is in equilibrium between open and closed conformations. In the absence of actin, the closed conformation is favored. When myosin binds actin, the open conformation becomes more favored, facilitating nucleotide release. We found that faster myosins favor a more closed pocket in the actomyosin•ADP state, with smaller values of ΔH^0 and ΔS^0, even though these myosins release ADP at a faster rate. A model involving a partitioning of free energy between work-generating steps prior to rate-limiting ADP release explains both the unexpected correlation between velocity and opening of the pocket and the observation that fast myosins are less efficient than slow myosins.

Introduction

Different members of the myosin superfamily move along actin filaments with widely varying velocities. This difference was first characterized in the case of skeletal muscle myosin. Skeletal muscles can be broadly classified into two types: slow-twitch (type I) fibers and fast-twitch (type II) fibers. The type I fibers have three to five times slower velocities and lower isometric ATPase activities than do the

*Corresponding author. Department of Biochemistry and Biophysics, UCSF MC 2240, Genentech Hall Room S416C, 600 16th Street, San Francisco, CA 94158-2517, USA.
E-mail address: tpurcell.phd@gmail.edu.

Abbreviations used: EPR, electron paramagnetic resonance; IFM, insect flight muscle; SLADP, spin-labeled ADP.

0022-2836/$ - see front matter © 2010 Elsevier Ltd. All rights reserved.

type II fibers.[1,2] The type I fibers are also more fatigue resistant than type II fibers.[3,4] A similar phenomenon is observed in cardiac muscles where the ventricle fibers are slower than the atrial fibers.[5] Smooth muscles are generally slower than skeletal or cardiac muscles.[6] Myosins from insect flight muscles (IFMs) on the other hand are very fast.[7] A vast difference in velocity is also observed in the non-muscle myosins. For example, mammalian myosin V has a relatively slow velocity, but some plant myosin XIs, while structurally similar to myosin V, can have velocities 2 orders of magnitude faster.[8,9] While the velocity of movement along actin filaments varies widely, the capacity to exert force is relatively constant in different myosins.[10] The ATPase activity varies, with the faster translation velocities associated with higher ATP turnover rates particularly when bearing high loads as seen in isometric contractions.[3] The tension cost, defined as the amount of ATP required to maintain tension for a given time, is thus much lower in slower myosins. Consequently, myosins have evolved to either move rapidly or maintain load economically.[11]

The difference in function between fast and slow muscle fibers is undoubtedly due to multiple isoforms of a number of different sarcomeric proteins.[2] The difference in fiber shortening velocity and probably also in isometric ATPase activity must be due in large part to differences in myosin isozymes, as the variations in fiber velocity are also found for filament translation by purified myosins, as reviewed in Ref. 12. The slower velocity observed for slower myosins is due to alterations in the rates of a number of reactions. However, there is evidence that a major determinant for velocity is the rate of release of ADP from the actin•myosin•ADP (A•M•ADP) complex near the end of the power stroke.[11,13] While other steps in the reaction cycle could limit ATPase, sliding velocity is limited by the slowest rate, k_{min}, in an attached state. Siemankowski *et al.* compared the rate of ADP dissociation in several different skeletal myosins and concluded that the measured ADP release rate from actomyosin (k_{-AD}) correlates closely to sliding velocity and is slow enough to be the rate-limiting step even in fast skeletal myosins.[13] Weiss *et al*. measured the rates of both ATP binding and ADP release and also concluded that, under physiological conditions, the ADP release rate k_{-AD} was sufficiently slow to be the limiting factor in shortening.[14]

Nyitrai *et al.* corrected for numerous systematic errors and again found a good correlation between k_{-AD} and sliding velocity.[11] They suggested a two-step mechanism for the release of ADP from actomyosin, A•M′•ADP ↔ A•M•ADP↔A•M +ADP, in which A•M′•ADP is assumed to be a state with a closed nucleotide pocket and A•M•ADP is open. Nyitrai and Geeves suggested that the closed pocket is favored in slower myosins, while the open state is favored in faster myosins.[15] If this transition is coupled with external force, it provides a mechanism for strain sensing or gating to efficiently conserve ATP in slower muscles.

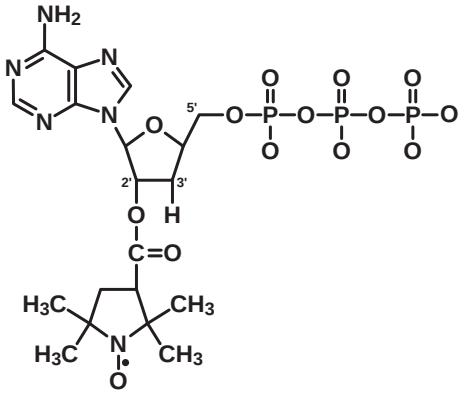

Fig. 1. The structure of 2′-spin-labeled ATP.

In this paper, we have explored conformational changes in myosin that are thought to be associated with the binding and release of nucleotides. As discussed above, the velocity of filament movement is determined by the rate of release of ADP, which is mediated by interaction of the myosin head with actin. By analogy with the G proteins,[16] the interaction with actin is transmitted to the nucleotide pocket by a region called switch 1. Electron paramagnetic resonance (EPR) spectroscopy using spin-labeled nucleotide analogs has been shown to be a useful method for monitoring movements of switch 1 in kinesin[17–19] and myosin.[20,21] For the spin probe employed, 2′-spin-labeled ADP (SLADP), the nitroxide spin label is attached at the 2′-hydroxy of the ribose ring in 3′-deoxyATP (Fig. 1). This probe binds at the nucleotide-binding site and is able to sense the surrounding conformation of the protein. Known movements of switch 1 would influence the mobility of the probe.

Nucleotide spin probes have shown decreased mobility when kinesin binds to microtubules and increased mobility when myosin binds to actin.[17,18,20] These results fit into the kinetic schemes of the two motors, with the closing of the kinesin nucleotide pocket promoting nucleotide hydrolysis and the opening of the myosin nucleotide pocket promoting product release. EPR spectroscopy using spin-labeled nucleotide demonstrates that the nucleotide pocket of fast skeletal muscle myosin has two conformations: a closed conformation favored in myosin alone and an open conformation that is favored upon the binding of myosin to actin. An open nucleotide pocket for myosin has also been shown by a variety of techniques. Myosin V crystal structures have shown that the upper 50-kDa domain can move, closing the prominent cleft in the 50-kDa domain and moving switch 1 to produce

Please cite this article as: Purcell, T. J. *et al.*, Nucleotide Pocket Thermodynamics Measured by EPR Reveal How Energy Partitioning Relates Myosin Speed to Efficiency, *J. Mol. Biol.* (2011), doi:10.1016/j.jmb.2010.11.053

a more open conformation of the nucleotide pocket.[22] Reconstructions of electron micrographs of the actin•myosin complex have shown that this conformational change occurs when myosin binds to actin.[23]

An opening of the myosin nucleotide pocket upon binding to actin is also reported in myosin V,[24] smooth muscle myosin,[25] and *Dictyostelium* myosin II[26] and by a variety of other techniques reviewed in Ref. 27. Opening of the pocket has also been shown by a functional assay that showed that ATP analogs with large moieties attached to the gamma phosphate could still bind to myosin.[28] Together, these results strongly suggest that upon binding of myosin to actin, switch 1 opens, allowing more rapid binding and release of nucleotides. Furthermore, the spin-labeled nucleotide analogs have shown that the pocket is in equilibrium between open and closed forms in the actomyosin•ADP complex, with the open conformation favored at higher temperatures.[20]

Here, we have extended our previous EPR studies on the conformation of the nucleotide pocket of myosin to include myosins from both fast and slow muscle types as well as two non-muscle myosins. We have developed more sensitive techniques for quantitating the population of states, allowing direct observation of the thermodynamics of the closed-to-open transition. We show that, upon binding to actin, the equilibrium between the open and the closed conformations of the myosin nucleotide pocket correlates with the velocity of the myosin. To our surprise, the open conformation of the nucleotide site is favored more strongly in the slower myosin. The observation of a more open pocket in slower myosins is unexpected, as the slower myosins are known to bind ADP more strongly. In addition, we find that the values of ΔH^0 and $T\Delta S^0$ for the transition are greater for slower myosins. Here, we explain the EPR results in terms of a model of the actin–myosin–ADP states that reconciles the EPR observations with the kinetic data and connects both to the observed correlation between efficiency of doing work and myosin velocity.

Results

EPR results

Figure 2a shows representative EPR spectra of SLADP in the presence of slow skeletal myosin. Each spectral component contributes three lines. For the unbound probes in solution, the fast rotational motion produces spin narrowing, leading to three very sharp lines labeled P2, P3, and P4. When the probe binds to the protein, its rotational mobility is restricted by the protein surface and the spectral lines are broadened, leading to peaks at the low and high fields labeled P1 and P5, respectively. All probes contribute to the central peak P3. For slow skeletal myosin, shown in Fig. 2a, the main bound component has a P1–P5 splitting of 6.2 mT. This splitting was similar in the absence of actin for all myosins studied. The spectra can be modeled by rapid rotational diffusion within a cone of vertex angles defined by the protein surface.[29,30] The observed splitting for myosin is consistent with a cone angle of 35° (all values are given as half angles of the cone vertex).

In the presence of actin, the bound component has a more narrow P1–P5 splitting of 5.3 mT, indicating that the nucleotide pocket has opened, consistent with rotational diffusion within a more open cone with a vertex angle of 51° (Fig. 2a). Additionally, the spectra show that although the main low-field component is changing, the low-field component also retains a shoulder, indicating a mix of more and less mobile probes. This indicates equilibrium between open and closed conformations of the nucleotide site. Similar data were obtained using a panel of different myosins in the actomyosin complex. The low-field components of the different EPR spectra are shown in Fig. 2b.

Deconvolution

Deconvolution allows quantitative measurement of the occupancy of the closed and open components of an experimentally observed spectrum. Basis spectra representing open and closed myosin nucleotide pockets were obtained by differential subtraction. The number of available spectra for quantitative analysis varied with myosin isoform. Depending on the isoform, 16 to 81 spectra that had primarily open nucleotide pockets as reported by probe mobility were averaged together and then subtracted from 25 to 42 averaged spectra with a primarily closed bound nucleotide pocket. Slow myosins and fast myosins were partitioned into two groups to determine the open and closed basis spectra. This significantly reduced the noise in the fits relative to open and closed basis spectra determined using only a single isoform. For *Dictyostelium* myosin II, there were sufficient spectra that this isoform could be analyzed by itself. The normalized difference results in a spectrum that has no spectral intensity corresponding to the more mobile bound probes as estimated for peaks P1 and P5, which represent the open nucleotide pocket component. Instead, the difference spectrum has intensity from more immobile probes representing the closed nucleotide pocket component of the spectrum and also from the three sharp P2–P4 components from unbound probe free in solution. The inverse subtraction results in a spectrum

Please cite this article as: Purcell, T. J. *et al.*, Nucleotide Pocket Thermodynamics Measured by EPR Reveal How Energy Partitioning Relates Myosin Speed to Efficiency, *J. Mol. Biol.* (2011), doi:10.1016/j.jmb.2010.11.053

representing only the open nucleotide pocket and the unbound probe components. The bound fraction of each representative spectrum was calculated by comparison to unbound spin-labeled nucleotide EPR spectra obtained in the absence of protein. Experimental spectra were then fit by a least-squares minimization to a linear sum of the three basis spectra: open, closed, and free (see Methods for details).

The basis sets for the deconvolutions were obtained by averaging spectra taken at different temperatures. These were found to provide reasonable fits to the data taken at a variety of temperatures. However, at the lowest temperature, there is a small (~0.05 mT) increase in the splitting of the component representing the least mobile probes, and this resulted in an error function that was a little larger than at higher temperatures. To explore how this affected the values of ΔH^0 and $T\Delta S^0$, we obtained a basis set for fast skeletal myosin at 4 °C and used it to fit the data at 4 °C and to replot the van 't Hoff plot. This fit showed that the standard basis set described above gave a small change in the population of the closed state, leading to a 15% decrease in the reported value of ΔH^0. This change is within the inherent scatter of the experimental data and much smaller than the fivefold total range of ΔH^0 values. A similar lineshape change in the other myosins would lead to a similar underestimate in ΔH^0 for all of them. The use of a separate basis set derived for a single temperature for each isoform also introduced greater errors due to the limited number of spectra available to derive the set, and thus, a single basis set was used across all temperatures. To further address the goodness of the fits, we considered the effect of a 5% change in the fractions of the two spectral components. This resulted in a 2.5% change in the thermodynamic parameters, again, well within the experimental error.

Figure 3a and b shows representative fits. The relative weightings of the component spectra are at the top of each panel. The least-squares fits (red) are superimposed on the experimentally observed spectra (black). The gray line at the bottom of each panel is the residual showing the goodness of the fit. The EPR spectra are the first derivative of absorbance with respect to the magnetic field variable. Double integration of the component spectra then yields the fractional occupancies of the components.

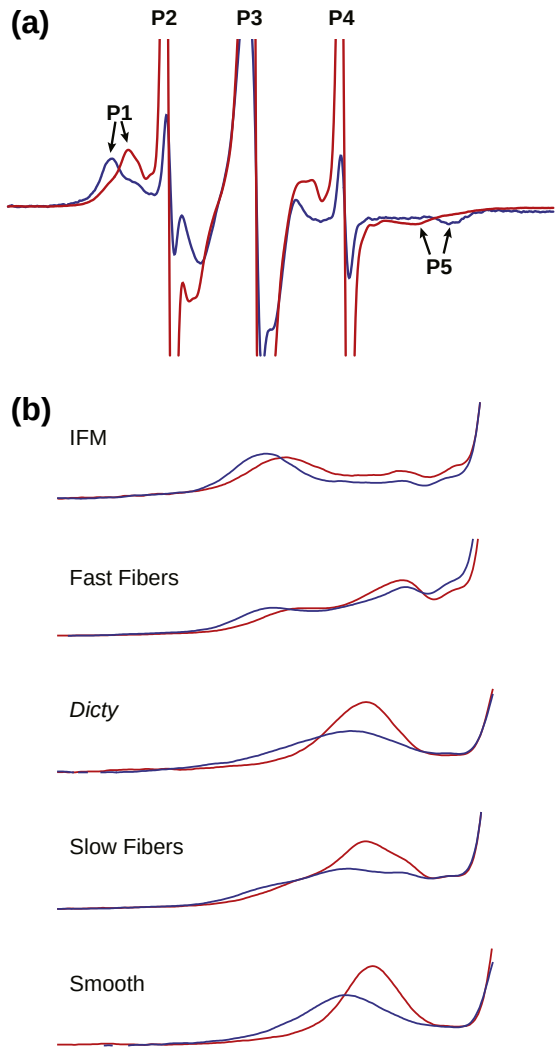

Fig. 2. (a) EPR spectra from rabbit slow skeletal myosin ± actin. The horizontal axis is magnetic field (10 mT wide with center field at 350 mT). The vertical axis is the derivative of absorbance. The blue trace shows 2′-SLADP with purified slow skeletal myosin in the absence of actin. The red trace is 2′-SLADP on slow skeletal fibers. Unbound spin-labeled nucleotide contributes to peaks P2, P3, and P4. Binding to myosin restricts the motion of the spin-labeled moiety, causing P2 to move downfield to P1 and P4 to move upfield to P5. The splitting of the outermost peaks is a function of the restriction of motion in the spin label, with the most restricted spin label seen in the absence of actin (blue trace). Binding to actin in the fibers causes the nucleotide pocket to open, resulting in P1 and P5 moving closer together as a result of the greater freedom of movement for the spin label. (b) Room temperature *versus* cold spectra. The low-field segment (P1 component) from room temperature spectra (22–24 °C, red traces) and cold spectra (2–4 °C, blue traces). In each case, at lower temperatures, there is greater amplitude on the left-hand side, representing decreased mobility of the nucleotide spin probe, implying that the fraction of myosin with a closed nucleotide pocket increases. This figure also shows the correlation for nucleotide pocket to the speed of the myosin. In the fastest myosins, IFM and fast skeletal muscle, the closed fraction is significantly populated even at room temperature, whereas the open fraction dominates slow myosins such as smooth and slow skeletal.

Please cite this article as: Purcell, T. J. *et al.*, Nucleotide Pocket Thermodynamics Measured by EPR Reveal How Energy Partitioning Relates Myosin Speed to Efficiency, *J. Mol. Biol.* (2011), doi:10.1016/j.jmb.2010.11.053

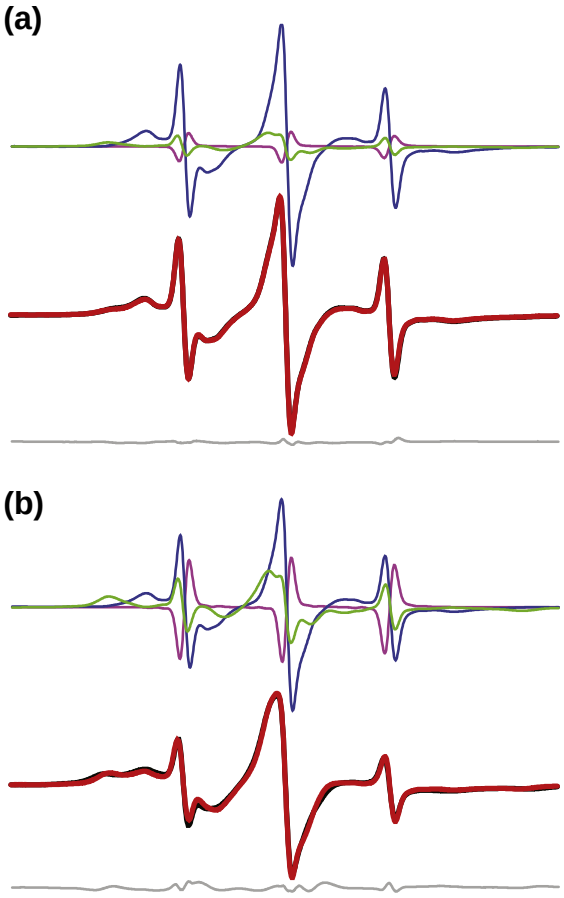

Fig. 3. Deconvolution of fast skeletal actomyosin. Representative spectra for closed (green), open (blue), and unbound (magenta) are summed to create a least-squares best-fit spectrum (red, middle panel) to the experimental spectrum (black, middle panel) with the residual shown in gray below. The open and closed representative spectra are a combination of bound and free spectra; thus, the pure free spectrum is actually subtracted in some cases to compensate for the fraction of free nucleotide in the experimental spectrum. (a) Room temperature and (b) 4 °C.

Once the population of each spectral component has been determined as described above, the equilibrium constant K_{eq} = [open fractional component of the spectrum]/[closed fractional component] can be determined from a single spectrum. Values of K_{eq} were used to calculate the free energy of the closed-to-open transition, $\Delta G^0 = -RT \ln K_{eq}$. Determination of ΔG^0 as a function of temperature was used to determine ΔH^0 and ΔS^0. Values for ΔG^0, below, are given at 25 °C.

Under most conditions, myosin with SLADP bound shows a mixture of open and closed states. In rabbit fast skeletal muscle myosin in the absence of actin, the closed form is favored, with a ΔG^0 for the closed-to-open transition of 2.0 ± 0.1 kJ mol^{-1}. In the presence of rabbit skeletal actin, the closed-to-open transition becomes favorable, with a ΔG^0 of -1.1 kJ mol^{-1}.

ΔG^0 correlation to speed

An advantage of using spin-labeled nucleotides is that they can be used in any myosin that can be obtained in sufficient quantities for EPR spectroscopy. Rabbit slow skeletal myosin also showed a closed nucleotide pocket in the absence of actin ($\Delta G^0 = 1.9$ kJ mol^{-1}). For slow actomyosin, the open nucleotide pocket state becomes greatly favored, $\Delta G^0 = -3.9$ kJ mol^{-1}. Surprisingly, slow muscle with an unloaded sliding velocity of 1.6 μm s^{-1} has a greater propensity for an open conformation of the nucleotide pocket compared with fast skeletal myosin (4.7 μm s^{-1}[31]) (both values of velocity were measured using skinned rabbit skeletal muscle fibers). Because faster myosin has a faster ADP release rate, we anticipated that the open nucleotide pocket conformation would be more energetically favored rather than less occupied as seen in our data.

In order to see if an increased velocity was the key correlative factor for this observation, we extended our analysis to other myosins with a range of speeds. We examined pig cardiac muscle, including atrial (fast, 2.7 μm s^{-1}[5]) and ventricle (slow, 1.3 μm s^{-1}[5]). These tissues recapitulated the trend seen in fast and slow skeletal muscles, with the ΔG^0 for fast atrial at -1.9 kJ mol^{-1} and slow ventricle at -3.9 kJ mol^{-1}. Smooth muscle from chicken gizzard is slower (0.67 μm s^{-1})[32] than slow skeletal and cardiac. Purified chicken gizzard myosin bound to actin shows a very open nucleotide pocket with a ΔG^0 of -3.8 kJ mol^{-1}. Similar results were obtained in expressed recombinant motor domain with essential light chain alone bound to actin. The correlation extends to faster muscle myosins as well. Even in the actomyosin state, in *Drosophila melanogaster* indirect flight muscle (*in vitro* motility of 6.4 μm s^{-1}[33]), the ΔG^0 for the closed-to-open transition is $+2.9$ kJ mol^{-1}.

In addition, we looked at non-muscle myosins. For velocity, we used the *in vitro* motility rate as an analogue of unloaded sliding velocity. Baculovirus expressed chicken myosin V is a slow myosin with an *in vitro* motility rate of 0.3 μm s^{-1},[8] and it has an open nucleotide pocket when bound to actin, $\Delta G^0 = -3.9$ kJ mol^{-1}. Expressed *Dictyostelium* myosin II is intermediate between fast and slow skeletal myosins [2.4 μm s^{-1} (average value from Refs. 34 and 35)] and has an intermediate ΔG^0 of -2.4 kJ mol^{-1} favoring the open nucleotide pocket.

Thus, the degree that the nucleotide pocket stays closed in the actomyosin state correlates to sliding velocity (Fig. 4). There are several factors that contribute to the sliding velocity for a given myosin,

Please cite this article as: Purcell, T. J. *et al.*, Nucleotide Pocket Thermodynamics Measured by EPR Reveal How Energy Partitioning Relates Myosin Speed to Efficiency, *J. Mol. Biol.* (2011), doi:10.1016/j.jmb.2010.11.053

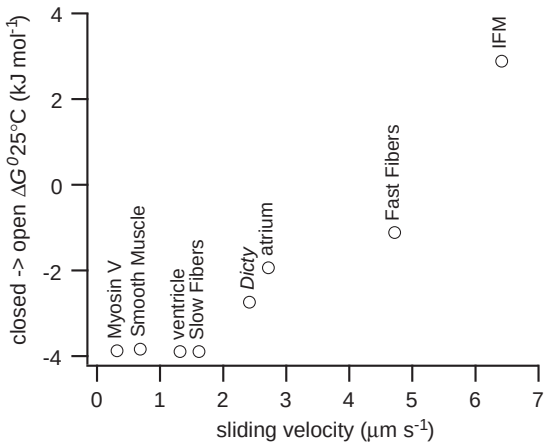

Fig. 4. ΔG^0 *versus in vitro* motility. The equilibrium between closed and open nucleotide pockets calculated from EPR data for a range of myosins from slow myosin V to fast IFM. Velocities are at room temperature (22–25 °C), taken from fiber shortening for fast and slow muscles,[31] cardiac muscle,[5] and smooth muscle;[32] where fiber shortening velocities are not available, *in vitro* sliding actin filament assay values were used for myosin V,[8] *Dictyostelium* myosin,[34,35] and IFM.[33]

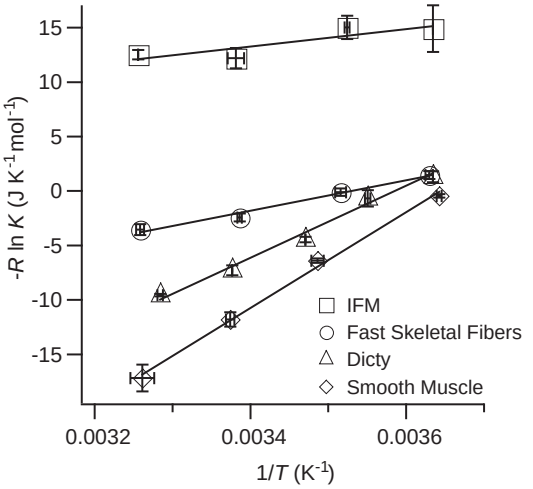

Fig. 5. Representative van 't Hoff plots. Data for the closed-to-open transition equilibrium (K) are fit by $-R \ln K = \Delta H^0 (1/T) - \Delta S^0$. The fits show that both ΔH^0 and ΔS^0 increase going from faster IFM and fast skeletal fibers to slower *Dictyostelium* and smooth muscle myosins. Error bars give the standard error of the mean for each group of data points with approximately 6 data points per observation.

including lever arm length and other rate-limiting steps, which could account for the deviation from a linear relationship. However, as we show below, the data suggest a model in which the nucleotide pocket reflects the energy of the actomyosin•ADP (A•M•D) complex and should correlate to the thermodynamics of this complex formation.

Temperature variation gives ΔH^0 and $T\Delta S^0$

The closed-to-open transition is temperature sensitive. For all of the myosins studied, the equilibrium of the actomyosin complex shifts back to favor the closed conformation (Fig. 2b) as the temperature is lowered. We measured the equilibrium constant as a function of temperature for each of the myosins studied. Plotting the log of the equilibrium constant as a function of reciprocal temperature yields the entropic and enthalpic components by a fit to the linear equation $-R \ln K = \Delta H^0 T^{-1} - \Delta S^0$ (Fig. 5). The magnitudes of ΔH^0 and ΔS^0 indicate a significant conformational change (Table 1). For example, the values are of the same magnitude as observed for kinesin neck linker undocking.[36] Naber *et al.* showed a much larger ΔH^0 (79 kJ mol^{-1}) and ΔS^0 (280 J K^{-1} mol^{-1}) for fast skeletal acto-S1.[20] However, those values were from S1 and an earlier version of the temperature control that had calibration issues. The exact nature of the conformational change is difficult to determine from these experiments, whether it's dynamics in the myosin–actin interface or dynamics within the myosin itself.

Discussion

Our previous work with spin-labeled nucleotides has shown that the mobility of bound probes increases when myosin binds to actin, implying that the nucleotide pocket of myosin adopts a more open conformation.[20] We have interpreted our spectral changes in terms of opening and closing of the switch 1 region because this is the region with known structural changes that would be in a position to influence the mobility of our ribose-bound probe.[28] Known movements of switch 2 would not alter probe mobility. As discussed in Introduction, a variety of techniques agree that the nucleotide pocket of myosin opens upon binding to actin.[20–22,24,26,27,37]

Table 1

Myosin	Sliding velocity (μm/s)	ΔG^0 25 °C (kJ mol^{-1})[a]	ΔH^0 (kJ mol^{-1})	ΔS^0 (J mol^{-1} K^{-1})
IFM	6.4	+2.9±0.1	10.4±3.6	25±12
Fast skeletal	4.7	−1.1±0.2	17.7±2.8	63±10
Atrial	2.7	−1.9±0.1	25.5±5.3	92±2
Dictyostelium	2.4	−2.7±0.2	44.1±1.7	157±5
Slow skeletal	1.6	−3.9±0.2	50.4±2.2	182±8
Ventricle	1.3	−3.9±0.2	55.5±9.0	199±31
Smooth	0.7	−3.8±0.1	43.9±0.1	160±1
Myosin V	0.3	−3.9±0.1	50.1±2.0	181±7

[a] Extrapolated from van 't Hoff plot.

Please cite this article as: Purcell, T. J. *et al.*, Nucleotide Pocket Thermodynamics Measured by EPR Reveal How Energy Partitioning Relates Myosin Speed to Efficiency, *J. Mol. Biol.* (2011), doi:10.1016/j.jmb.2010.11.053

Our previous results showing an opening of the nucleotide pocket upon binding to actin support our findings in light of the structural interpretation above. The bond with actin promotes release of phosphate first and, subsequently, ADP. Release of ADP would be expected to be enhanced by an open conformation of the nucleotide pocket, weakening the association of ADP. This has been postulated to be the state from which ADP is released in previous kinetic models.[38] Furthermore, a greater population of the open state could be expected to promote more rapid release of ADP, as has also been postulated in previous kinetic models.[38] Thus, the present results, which show that the more open form is favored in slower myosins, is counterintuitive. One would expect slower myosins to favor the closed form to slow the release of ADP. However, we note that the rate of release of ADP is not always correlated with the switch 1 conformation. X-ray structures of kinesin and nonclaret disjunctional protein show an extremely open switch 1 coupled with very tight binding and a very slow release rate of ADP. Release of nucleotides from G-proteins is associated with alterations at the nucleotide site in the P-loop and switch regions by guanine exchange factors.[39]

Our observation that actomyosin•ADP has multiple conformational states is consistent with other kinetic and spectroscopic studies for several myosins studied here, including myosin V,[40,41] smooth muscle myosin II,[42] and *Dictyostelium* myosin.[26] The kinetics of myosin V actomyosin•ADP are consistent with high- and low-affinity states as measured in Rosenfeld *et al*.[40] This could correspond to the open and closed states with a ΔG^0 at 20 °C of −3.0 kJ mol^{-1}. Hannemann *et al.* also measured a similar apparent equilibrium between high- and low-affinity states, −3.3 kJ mol^{-1} at 25 °C.[41] Both of these values are close to the equilibrium observed in EPR of −3.0 kJ mol^{-1} and −3.9 kJ mol^{-1} for 20 °C and 25 °C, respectively. In the absence of actin, the Hannemann equilibrium $K_{isom,Mg}$ of +1.3 kJ mol^{-1} is close to what we observe with EPR in the absence of actin (+0.9 kJ mol^{-1}). This value for ΔG^0 is different from that measured by Rosenfeld (−1.9 kJ mol^{-1}), although both papers agree on the general observation that binding to actin results in a relative increase in the fraction of the open nucleotide pocket. Spectroscopic experiments with smooth muscle myosin II are also consistent with two fluorescent states in the actomyosin•mant-ADP state. At 20 °C, acto-S1•ADP has a ΔG^0 of −0.7 kJ mol^{-1} compared to our EPR-derived value of −3.0 kJ mol^{-1}. Rosenfeld *et al.* obtained a value strongly favoring the closed form, with a ΔG^0 of +7.6 kJ mol^{-1} in the absence of actin, which is greater than that found here.[42] They also found the entropy and enthalpy values by van 't Hoff analysis in the absence of actin. The ΔH^0 and ΔS^0 values were 44 kJ mol^{-1} and 123 J K^{-1} mol^{-1}, respectively, similar to our values of 44 kJ mol^{-1} and 160 J K^{-1} mol^{-1} that were calculated for actomyosin and 32 kJ mol^{-1} and 109 J K^{-1} mol^{-1} for myosin.

Fluorescence spectroscopy experiments with *Dictyostelium* myosin also showed evidence for two A•M•ADP states.[26] Using a construct with a single tryptophan mutant, F239W, in a tryptophan-free background, they found a ΔG^0 of +0.8 kJ mol^{-1} for ADP binding in the absence of actin at 12 °C, close to our own value of +1.0 kJ mol^{-1} measured by EPR spectroscopy using the same mutant. In summary, there are a variety of techniques that agree that the myosin nucleotide pocket has two conformations, with reasonable agreement in the magnitude of the energetic differences between them, given the uncertainties in the methods.

A model to explain the correlation between ΔG^0 and velocity

Below, we discuss a model that can explain the unexpected relationship between the open and the closed conformations of the nucleotide pocket and ADP release. As with previous models, ADP release occurs only from the open state. In previous models, the rate-limiting state in ADP release was the transition from the closed to the open state. Once in the open state, ADP release was fast. If instead, the rate-limiting step is placed between the open state and the rigor state and the free energy of the open state is varied while keeping the free energies of the closed and ADP release transition states fixed, the correlation between velocity and ΔG^0 can be explained. The lower the free energy of the open state relative to the closed state, the more the open conformation of the nucleotide pocket is favored. As seen in Fig. 6, slow myosin (red) has a lower energy state than the fast myosin (blue) in the A•M^{open}•D state. The greater ΔG^0 between the open state and the transition state results in a slower release of ADP, assuming that the ADP-releasing transition state A•M‡–D is similar in energy for faster and slower myosins. We further show below that this model explains the correlation between ΔG^0 and velocity and makes a connection between both of these observations and the efficiency of performing mechanical work.

As discussed in Introduction, there is a reasonable inverse correlation between the velocity and the affinity of ADP for the actomyosin complex K_{AD}.[11] Our own measurements, however, relate not directly to the affinity of ADP but to the relative energies of the A•M•ADP states, A•M•ADP states, A•M^{closed}•D and A•M^{open}•D, in Fig. 6. The four affinities defining the binding of actin, myosin, and ADP to form the aggregate A•M•ADP state are related by virtue of being involved in a closed thermodynamic box (top panel, Fig. 7a). The thermodynamic box defines the association constants K_D, K_A, K_{AD}, and K_{DA}.

Please cite this article as: Purcell, T. J. *et al.*, Nucleotide Pocket Thermodynamics Measured by EPR Reveal How Energy Partitioning Relates Myosin Speed to Efficiency, *J. Mol. Biol.* (2011), doi:10.1016/j.jmb.2010.11.053

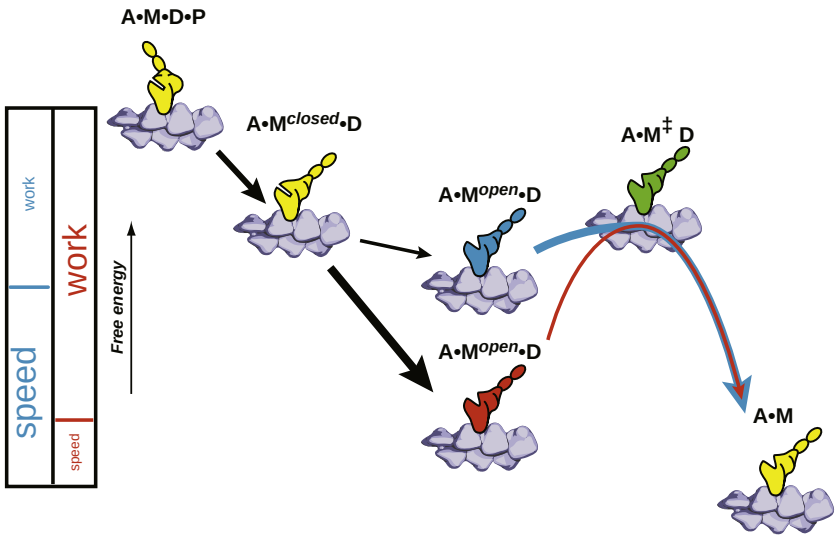

Fig. 6. Energy diagram. Slow myosin (red) has a lower energy state than the fast myosin (blue) in the A•M^{open}•D state. The greater ΔG^0 causes a slower release of ADP, assuming that the ADP-releasing transition state A•M‡–D is similar in energy for faster and slower myosins. The relationship between speed and efficiency is illustrated by the partitioning between two phases. The steps up to the A•M^{open}•D state contribute to the work output of the myosin; the large free-energy drop in the slower myosin allows a greater portion of the free energy to be used for work, resulting in a more efficient myosin. The faster myosin budgets less energy for the work phases of the stroke but has a greater fraction of energy left over to drive nucleotide release, resulting in a faster but less efficient myosin.

The values most directly associated with the A•M•ADP state, K_{AD} and K_{DA}, have a stronger correlation with the velocity of the myosin since they modulate the fraction of myosin in the bound actomyosin–diphosphate state. The coupling coefficient is a measure of the reduction of K_{AD} and K_{DA} compared to K_D and K_A. Slow myosins have a lower coupling coefficient, indicating that ADP affinity is high, with or without actin, and actin affinity is high, with or without ADP. On the other hand, the coupling coefficient is high in fast myosins, indicating that ADP binding is destabilized in actomyosin relative to myosin. If one assumes, arbitrarily, that the free energy of the A•M^{closed}•D state (Fig. 6) is reasonably constant with velocity, and with the A•M‡•D transition-state intermediate only sparsely populated, then changes in the free energy of the A•M^{open}•D state will determine the overall free energy of the aggregate A•M•D state and the overall affinity of actomyosin to ADP. If the other states (M, A•M, and M•D) were relatively constant in energy, this would indicate that the A•M•ADP state is specifically destabilized in faster myosins. This is represented diagrammatically in Fig. 7b by the tilting of the thermodynamic boxes with respect to the vertical free-energy axis. Comparing the red and blue boxes, the red box vertex representing the A•M•D^{slow} myosin isoform is of lower free energy than the corresponding vertex in the blue box representing the A•M•D^{fast} isoform. In other words, the decrease in free energy associated with the formation of the A•M•ADP complex (i.e., the A•M^{closed}•D-to-A•M^{open}•D transition) becomes greater as the velocity decreases for the slower isoform.

As shown in Figs. 6 and 7, the free energy experimentally measured here, ΔG^0, reports on the change in energy between the two lowest states of the A•M•ADP complex: A•M^{closed}•D to A•M^{open}•D. As noted above, if the free energy of A–M^{closed}–D is reasonably constant with velocity, then changes in the free energy of the A•M^{open}•D state will determine the overall free energy of the A•M•D state and overall affinity of actomyosin to ADP. Thus, the relationship between the change in free energy and the equilibrium constant between the A•M^{closed}•D and the A•M^{open}•D states and the fact that the transition out of the A•M^{open}•D state is rate limiting for sliding velocity imply that the log of the velocity would correlate inversely to the stabilization of the open state. Thus, this model explains three things: (1) the pocket is more open in slower myosins, (2) the affinity of ADP for the A•M complex is greater, and (3) a greater amount of energy is released in the formation of the A•M•ADP complex. This last quantity can further be related to muscle efficiency, as discussed below.

We also note that the slower myosins are associated with greater values of ΔH^0 and $T\Delta S^0$. The magnitude of the change is great, amounting to over a fivefold difference between the fastest myosin, $\Delta H^0 = 10$ kJ mol^{-1}, and the slowest myosin, $\Delta H^0 = 50$ kJ mol^{-1}. As noted in the Methods section,

Please cite this article as: Purcell, T. J. *et al.*, Nucleotide Pocket Thermodynamics Measured by EPR Reveal How Energy Partitioning Relates Myosin Speed to Efficiency, *J. Mol. Biol.* (2011), doi:10.1016/j.jmb.2010.11.053

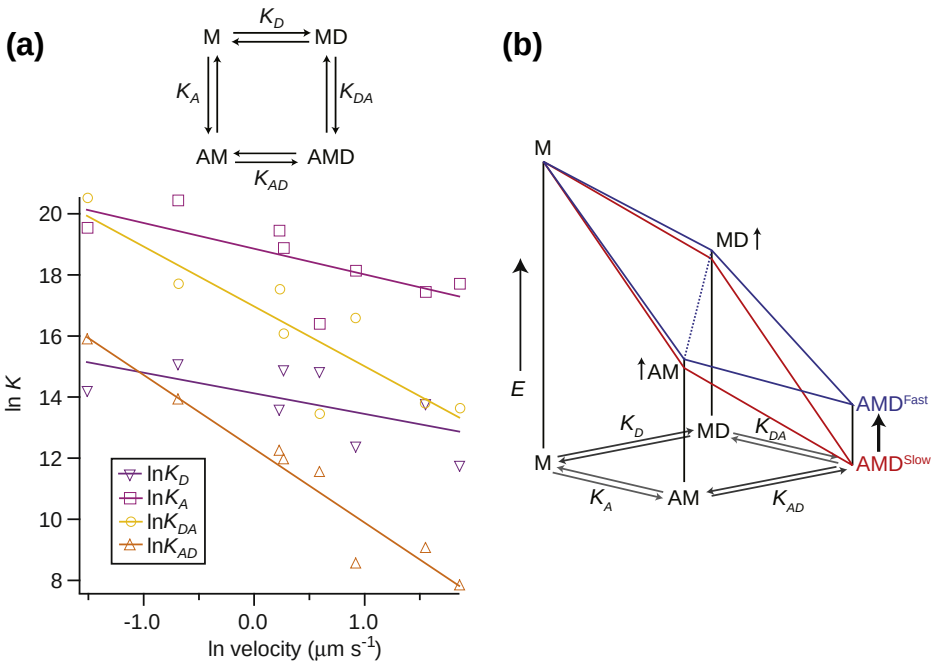

Fig. 7. (a) Equilibrium constant *K versus* velocity. Association equilibrium constants estimated from published values for the closed thermodynamic box (after Ref. 15). The box represents two paths from myosin to actomyosin•ADP, and in both cases, the second step has a stronger influence on myosin sliding speed. *K* values are taken from the literature. From slowest to fastest, the myosins are human non-muscle myosin IIB,[43] chicken myosin V,[44] chicken gizzard smooth muscle myosin II,[45] *Dictyostelium* myosin II,[46] bovine ventricle cardiac myosin II, rabbit slow skeletal muscle (*soleus*) myosin II,[47] rabbit fast skeletal (*psoas*) myosin II,[11] and *Drosophila* flight muscle.[33,48] Affinities at 100 mM KCl were estimated from published values using the equation log $K \propto 5 \times \sqrt{\text{ionic strength}}$[49] and corrected to 25 °C using the published temperature dependence.[50] (b) Energy landscape for the closed thermodynamic box for slow *versus* fast myosins. Data from the graph showing the energy difference between fast (blue) and slow (red) myosins are from the estimated *K* values corresponding to 0.3 μm s^{-1} for slow myosins and 7 μm s^{-1} for fast myosins. Vertical axis scales the relative energy difference proportional to log *K*. Setting the energy for the myosin state as the reference, there is only a modest difference between slow and fast myosins in the A•M and M•D states. However, there is a large difference in the A•M•D state resulting in a kinked box for fast myosins (blue). The energy landscape for a fast myosin has a kink in the middle, indicating that the coupling constant relates specifically to destabilization of the A•M•D state.

the changes in lineshape that occur with temperature lead to a 15% underestimate in the values of ΔH^0 for all myosins. If changes in ΔH^0 and $T\Delta S^0$ reflect alteration in the size of the protein interface formed in the actomyosin complex, the observed correlations would suggest that a greater amount of protein–protein interface is formed in the open state of the pocket in slower myosins. It is possible that this interface contributes to the lower free energy of the A•M•ADP complex. The collection of myosins at the lowest end of the speed range has approximately the same ΔG^0 for the closed-to-open equilibrium. There might no longer be a way to stabilize the A•M•ADP complex without equally affecting both A•M^{closed}•ADP and the A•M^{open}•ADP states.

Efficiency

There is evidence that the efficiency, defined as the percentage of the chemical energy available from ATP that is converted to mechanical work, is greater in slower fibers. This was first determined from a comparison of two vertebrate muscles: frog and tortoise fibers.[51] In particular, this can be seen upon comparison of different muscle types from a given organism or upon comparison of different isoforms from the same family. For example, mouse slow-twitch *soleus* was reported to have an efficiency of 43% compared to fast-twitch *extensor digitorum longus* with an efficiency of 33%.[52] A similar correlation is seen with fast and slow muscles of the chicken.[53] The efficiency of myosin V is estimated from *in vitro* measurements to approach 100%.[54] Myosin XI in tobacco yellow bright-2 cells is another processive myosin that is functionally and structurally similar to myosin V in that it takes 36-nm steps corresponding to the actin pseudo-repeat but has a velocity that is 20-fold faster than myosin V. For this myosin isoform, the efficiency drops down to 20%.[9] This correlation further extends across species from very slow muscles such as tortoise *rectus femoris*,

Please cite this article as: Purcell, T. J. *et al.*, Nucleotide Pocket Thermodynamics Measured by EPR Reveal How Energy Partitioning Relates Myosin Speed to Efficiency, *J. Mol. Biol.* (2011), doi:10.1016/j.jmb.2010.11.053

efficiency of 77%,[51] and myosin V, 80%,[8] to the fastest muscles considered here, *Drosophila* indirect flight muscle. *Drosophila* flight muscle (IFM) has an estimated efficiency of around 30%.[55] Significantly, extrapolating the correlation shown in Fig. 8 out to zero efficiency gives a theoretical maximum velocity for actomyosin of around 50 μm s^{-1}, which is on the order of the fastest observed sliding velocities from plant myosin XI.[56]

There is evidence that the stronger the A•M•ADP complex, the more energy is available to do work. A very large amount of free energy is released upon formation of this complex, and the high efficiencies of some myosins would require that a large fraction of this free energy be used to do work. A number of models have assumed that the energy released in formation of this complex is used to drive the production of mechanical work (Ref. 57 and references therein). Variation of the strength of the A•M•ADP complex has additionally shown that the isometric force is directly correlated to the free energy released by formation of the A•M•ADP complex.[58] Thus, the model above, which links slower velocities to a more open myosin nucleotide pocket and to a stronger A•M•ADP complex, would explain the correlation between efficiency and velocity. In this model, a partitioning of some subset of the total energy available between work (*W*) and ADP release would result in a negative correlation between the efficiency and the logarithm of sliding velocity. Figure 8 shows that, indeed, a very good fit is obtained, making the simplest possible assumption that the relationship between efficiency and logarithm of sliding velocity is linear.

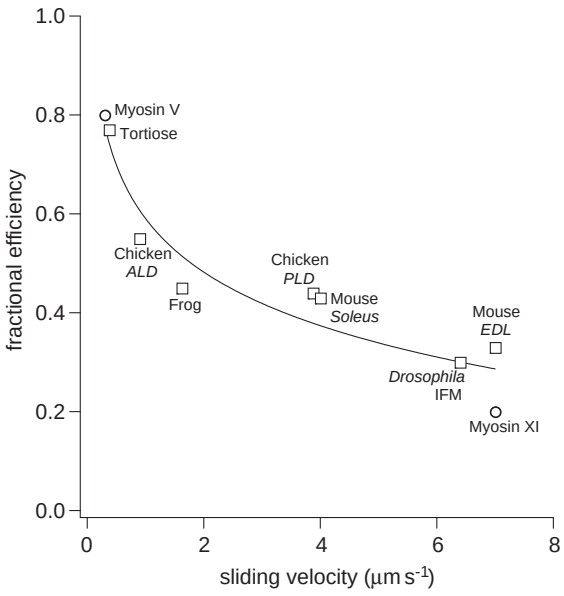

Fig. 8. Efficiency *versus* velocity. Fractional efficiencies for muscle (squares) and processive non-muscle (circles) myosins. The best least-squares fit is given by $eff = -1.6 \ln v + 0.59$, assuming a linear relationship between fractional efficiency (*eff*) and the logarithm of velocity (*v*). Muscles: tortoise *rectus femoris*,[51] chicken *anterior latissimus dorsi*,[53] frog *sartorius*,[51] chicken *posterior latissimus dorsi*,[53] mouse *soleus*,[52] *Drosophila* adult indirect flight muscle,[55] and mouse *extensor digitorum muscle*.[52] Non-muscles: MV chicken myosin V[54] and MXI tobacco yellow bright-2 cells myosin XI.[9]

Discussion summary

EPR spectroscopy using a spin-labeled nucleotide has resulted in structural information about the actomyosin•ADP state, a state that has not been studied by X-ray crystallography. Furthermore, quantitative analysis results in thermodynamic information about this state, confirming equilibrium between open and closed conformations of the nucleotide pocket. Because the spectroscopic probe was attached to a nucleotide that bound effectively to myosin, a panel of myosins with a greater than 20-fold range of sliding velocities could be studied, resulting in the counterintuitive result that the open-nucleotide-pocket state is favored in myosins that slowly release ADP, even though ADP release is thought to occur from the open conformation. Our analysis suggests that destabilization of the open actomyosin ADP state in faster myosins lowers the free-energy barrier for ADP release through a transition-state intermediate, resulting in faster ADP release. This destabilization comes at the cost of work-producing transitions leading up to the opening of the nucleotide-binding pocket. This model results in a simplified thermodynamic model for the relationship between speed and efficiency in myosin-based motility.

Methods

Protein preparations

F-actin was purified from rabbit skeletal muscle.[59] The *Dictyostelium discoideum* tryptophan-free M761 motor domain cDNA fragment was expressed in Dd AX2-ORF+ cells and isolated as described previously.[60] Cardiac atrial and ventricular myosins were isolated from porcine hearts using the protocols of Tonomura *et al.*[61] Chicken gizzard smooth muscle myosin was isolated following the protocols of Ikebe and Hartshorne.[62] Myosin V motor domain was expressed, harvested, and purified as in Sweeney *et al.*[63] Myosin subfragment-1 (S1) was prepared by chymotryptic digestion of myosin as described in Weeds and Taylor.[64]

Myosin fiber preparations

Fast (*psoas*) and slow (*soleus*) rabbit skeletal fibers were harvested and chemically skinned as described in Naber *et al.*[20] IFM fibers were dissected from a 2- to 3-day-old

Please cite this article as: Purcell, T. J. *et al.*, Nucleotide Pocket Thermodynamics Measured by EPR Reveal How Energy Partitioning Relates Myosin Speed to Efficiency, *J. Mol. Biol.* (2011), doi:10.1016/j.jmb.2010.11.053

female *Drosophila* and chemically skinned and stored as previously described, except that fibers were not split in half.[65] The demembranated fibers were used within 5 days.

Solutions

The basic rigor experimental buffer consisted of 5 mM $Mg(OAc)_2$, 1 mM ethylene glycol bis(β-aminoethyl ether) *N*,*N*′-tetraacetic acid, and 40 mM 4-morpholinepropanesulfonic acid, pH 7.0. For experiments involving skinned fibers, 50 mM KOAc was added to the rigor buffer.

EPR spectroscopy

For experiments with S1 or expressed motor domain, with or without actin present, protocols for spin labeling and mounting the protein in a capillary for EPR spectral accumulation were as in Naber *et al.*[20] IFM fibers were washed in a 500-fold excess (v/v) of rigor buffer and isolated via centrifugation to eliminate the DTT present in the glycerination and storage buffers. The process was repeated four times. Rabbit *psoas* and *soleus* fibers were minced with a razor blade for EPR spectroscopy experiments. The fiber preparation was then spin labeled and mounted on a flat cell for spectral accumulation as described in Naber *et al.*[20] EPR measurements were performed with a Bruker EMX EPR spectrometer (Billerica, MA). First-derivative X-band spectra were recorded in a high-sensitivity microwave cavity using 50-s, 10-mT-wide magnetic field sweeps. The instrument settings were as follows: microwave power, 25 mW; time constant, 164 ms; frequency, 9.83 GHz; and modulation, 0.1 mT at a frequency of 100 kHz. Each spectrum used in data analysis was an average of 5–50 sweeps from an individual experimental preparation. Temperature was controlled by blowing dry air (warm or cool) into the cavity and monitored using a thermistor placed close to the experimental sample. Effective cone angles of mobility were determined following Griffith and Jost and Alessi *et al.*[29,30]

Deconvolution of spectral components

The goal is to represent the experimentally observed spectrum as a linear combination of three basis spectra. The basis spectra are the spectral components from the open conformation of the nucleotide pocket, the closed conformation of the nucleotide pocket, and unbound probe free in solution. Each spectrum is discretized into 1024 individual data pairs with a cubic spline interpolation used to align the data points. Let O_i, C_i, F_i, and E_i, $i=1.1024$, be the discretized open, closed, unbound probe free in solution, and experimentally observed spectra. Then the relative weighting of the three individual open, closed, and free spectra will be given by the constants, *A*, *B*, and *C* that minimize

$$\sum_{i=1}^{1024}(AO_i + BC_i + CF_i - E_i)^2$$

(least-squares minimization). The minimization was done using the Matlab V7.8 routine fminsearch (Nelder–Mead simplex method) with a convergence criteria of 0.0001 for TolFun and TolX. Then $AO_i+BC_i+CF_i$, $i=1.1024$, is the least-squares fit to the experimentally determined spectrum.

Acknowledgements

This work was supported by National Institutes of Health grants HL032145 (T.J.P. and K.F.-S.), AR042895 (R.C. and N.N.), GM077067 (E.P. and N.N.), AR055611 (D.M.S. and C.C.E.), HL063798 (C.L.B.), and GM33289 (J.S.), Burroughs Wellcome Career Award at the Scientific Interface, American Heart Association Postdoctoral Fellowship, Jane Coffin Childs Postdoctoral Fellowship (A.R.D.), and the European Research Council IDEAS forcemap (208319) (A.M.-C.).

References

1. Bottinelli, R., Betto, R., Schiaffino, S. & Reggiani, C. (1994). Unloaded shortening velocity and myosin heavy chain and alkali light chain isoform composition in rat skeletal muscle fibres. *J. Physiol.* **478**, 341–349.
2. Weiss, A. & Leinwand, L. A. (1996). The mammalian myosin heavy chain gene family. *Annu. Rev. Cell Dev. Biol.* **12**, 417–439.
3. Bottinelli, R., Canepari, M., Reggiani, C. & Stienen, G. J. (1994). Myofibrillar ATPase activity during isometric contraction and isomyosin composition in rat single skinned muscle fibres. *J. Physiol.* **481**, 663–675.
4. Fitts, R. H. (1994). Cellular mechanisms of muscle fatigue. *Physiol. Rev.* **74**, 49–94.
5. Malmqvist, U. P., Aronshtam, A. & Lowey, S. (2004). Cardiac myosin isoforms from different species have unique enzymatic and mechanical properties. *Biochemistry*, **43**, 15058–15065.
6. Arner, A., Lofgren, M. & Morano, I. (2003). Smooth, slow and smart muscle motors. *J. Muscle Res. Cell Motil.* **24**, 165–173.
7. Swank, D. M., Vishnudas, V. K. & Maughan, D. W. (2006). An exceptionally fast actomyosin reaction powers insect flight muscle. *Proc. Natl Acad. Sci. USA*, **103**, 17543–17547.
8. Mehta, A. D., Rock, R. S., Rief, M., Spudich, J. A., Mooseker, M. S. & Cheney, R. E. (1999). Myosin-V is a processive actin-based motor. *Nature*, **400**, 590–593.
9. Tominaga, M., Kojima, H., Yokota, E., Orii, H., Nakamori, R., Katayama, E. *et al.* (2003). Higher plant myosin XI moves processively on actin with 35 nm steps at high velocity. *EMBO J.* **22**, 1263–1272.
10. Stienen, G. J., Kiers, J. L., Bottinelli, R. & Reggiani, C. (1996). Myofibrillar ATPase activity in skinned human skeletal muscle fibres: fibre type and temperature dependence. *J. Physiol.* **493**, 299–307.
11. Nyitrai, M., Rossi, R., Adamek, N., Pellegrino, M. A., Bottinelli, R. & Geeves, M. A. (2006). What limits the velocity of fast-skeletal muscle contraction in mammals? *J. Mol. Biol.* **355**, 432–442.

Please cite this article as: Purcell, T. J. *et al.*, Nucleotide Pocket Thermodynamics Measured by EPR Reveal How Energy Partitioning Relates Myosin Speed to Efficiency, *J. Mol. Biol.* (2011), doi:10.1016/j.jmb.2010.11.053

12. Bottinelli, R. (2001). Functional heterogeneity of mammalian single muscle fibres: do myosin isoforms tell the whole story? *Pfluegers Arch.* **443**, 6–17.
13. Siemankowski, R. F., Wiseman, M. O. & White, H. D. (1985). ADP dissociation from actomyosin subfragment 1 is sufficiently slow to limit the unloaded shortening velocity in vertebrate muscle. *Proc. Natl Acad. Sci. USA*, **82**, 658–662.
14. Weiss, S., Rossi, R., Pellegrino, M. A., Bottinelli, R. & Geeves, M. A. (2001). Differing ADP release rates from myosin heavy chain isoforms define the shortening velocity of skeletal muscle fibers. *J. Biol. Chem.* **276**, 45902–45908.
15. Nyitrai, M. & Geeves, M. A. (2004). Adenosine diphosphate and strain sensitivity in myosin motors. *Philos. Trans. R. Soc. London, Ser. B*, **359**, 1867–1877.
16. Vetter, I. R. & Wittinghofer, A. (2001). The guanine nucleotide-binding switch in three dimensions. *Science*, **294**, 1299–1304.
17. Naber, N., Minehardt, T. J., Rice, S., Chen, X., Grammer, J., Matuska, M. *et al.* (2003). Closing of the nucleotide pocket of kinesin-family motors upon binding to microtubules. *Science*, **300**, 798–801.
18. Wong, Y. L., Dietrich, K. A., Naber, N., Cooke, R. & Rice, S. E. (2009). The Kinesin-1 tail conformationally restricts the nucleotide pocket. *Biophys. J.* **96**, 2799–2807.
19. Larson, A. G., Naber, N., Cooke, R., Pate, E. & Rice, S. E. (2010). The conserved L5 loop establishes the pre-powerstroke conformation of the Kinesin-5 motor, eg5. *Biophys. J.* **98**, 2619–2627.
20. Naber, N., Purcell, T. J., Pate, E. & Cooke, R. (2007). Dynamics of the nucleotide pocket of myosin measured by spin-labeled nucleotides. *Biophys. J.* **92**, 172–184.
21. Naber, N., Malnasi-Csizmadia, A., Purcell, T. J., Cooke, R. & Pate, E. (2010). Combining EPR with fluorescence spectroscopy to monitor conformational changes at the myosin nucleotide pocket. *J. Mol. Biol.* **396**, 937–948.
22. Coureux, P. D., Sweeney, H. L. & Houdusse, A. (2004). Three myosin V structures delineate essential features of chemo-mechanical transduction. *EMBO J.* **23**, 4527–4537.
23. Holmes, K. C., Angert, I., Kull, F. J., Jahn, W. & Schroder, R. R. (2003). Electron cryo-microscopy shows how strong binding of myosin to actin releases nucleotide. *Nature*, **425**, 423–427.
24. Sun, M., Oakes, J. L., Ananthanarayanan, S. K., Hawley, K. H., Tsien, R. Y., Adams, S. R. & Yengo, C. M. (2006). Dynamics of the upper 50-kDa domain of myosin V examined with fluorescence resonance energy transfer. *J. Biol. Chem.* **281**, 5711–5717.
25. Robertson, C. I., Gaffney, D. P., II, Chrin, L. R. & Berger, C. L. (2005). Structural rearrangements in the active site of smooth-muscle myosin. *Biophys. J.* **89**, 1882–1892.
26. Kintses, B., Gyimesi, M., Pearson, D. S., Geeves, M. A., Zeng, W., Bagshaw, C. R. & Malnasi-Csizmadia, A. (2007). Reversible movement of switch 1 loop of myosin determines actin interaction. *EMBO J.* **26**, 265–274.
27. Malnasi-Csizmadia, A., Dickens, J. L., Zeng, W. & Bagshaw, C. R. (2005). Switch movements and the myosin crossbridge stroke. *J. Muscle Res. Cell Motil.* **26**, 31–37.
28. Pate, E., Naber, N., Matuska, M., Franks-Skiba, K. & Cooke, R. (1997). Opening of the myosin nucleotide triphosphate binding domain during the ATPase cycle. *Biochemistry*, **36**, 12155–12166.
29. Griffith, O. H. & Jost, P. C. (1976). Lipid spin labels in biological membranes. In (Berlinger, L. J., ed.), Academic Press, New York, NY.
30. Alessi, D. R., Corrie, J. E., Fajer, P. G., Ferenczi, M. A., Thomas, D. D., Trayer, I. P. & Trentham, D. R. (1992). Synthesis and properties of a conformationally restricted spin-labeled analog of ATP and its interaction with myosin and skeletal muscle. *Biochemistry*, **31**, 8043–8054.
31. Cuda, G., Pate, E., Cooke, R. & Sellers, J. R. (1997). *In vitro* actin filament sliding velocities produced by mixtures of different types of myosin. *Biophys. J.* **72**, 1767–1779.
32. Warshaw, D. M., Desrosiers, J. M., Work, S. S. & Trybus, K. M. (1990). Smooth muscle myosin cross-bridge interactions modulate actin filament sliding velocity *in vitro*. *J. Cell Biol.* **111**, 453–463.
33. Swank, D. M., Knowles, A. F., Kronert, W. A., Suggs, J. A., Morrill, G. E., Nikkhoy, M. *et al.* (2003). Variable N-terminal regions of muscle myosin heavy chain modulate ATPase rate and actin sliding velocity. *J. Biol. Chem.* **278**, 17475–17482.
34. Kron, S. J. & Spudich, J. A. (1986). Fluorescent actin filaments move on myosin fixed to a glass surface. *Proc. Natl Acad. Sci. USA*, **83**, 6272–6276.
35. Uyeda, T. Q., Abramson, P. D. & Spudich, J. A. (1996). The neck region of the myosin motor domain acts as a lever arm to generate movement. *Proc. Natl Acad. Sci. USA*, **93**, 4459–4464.
36. Rice, S., Cui, Y., Sindelar, C., Naber, N., Matuska, M., Vale, R. & Cooke, R. (2003). Thermodynamic properties of the kinesin neck-region docking to the catalytic core. *Biophys. J.* **84**, 1844–1854.
37. Schröder, R. R., Manstein, D. J., Jahn, W., Holden, H., Rayment, I., Holmes, K. C. *et al.* (1993). Three-dimensional atomic model of F-acton decorated with *Dictyostelium* myosin S1. *Nature*, **364**, 171–174.
38. Geeves, M. A. & Holmes, K. C. (1999). Structural mechanism of muscle contraction. *Annu. Rev. Biochem.* **68**, 687–728.
39. Bos, J. L., Rehmann, H. & Wittinghofer, A. (2007). GEFs and GAPs: critical elements in the control of small G proteins. *Cell*, **129**, 865–877.
40. Rosenfeld, S. S., Houdusse, A. & Lee Sweeney, H. (2005). Magnesium regulates ADP dissociation from myosin V. *J. Biol. Chem.* **280**, 6072–6079.
41. Hannemann, D. E., Cao, W., Olivares, A. O., Robblee, J. P. & De La Cruz, E. M. (2005). Magnesium, ADP, and actin binding linkage of myosin V: evidence for multiple myosin V–ADP and actomyosin V–ADP states. *Biochemistry*, **44**, 8826–8840.
42. Rosenfeld, S. S., Xing, J., Whitaker, M., Cheung, H. C., Brown, F., Wells, A. *et al.* (2000). Kinetic and spectroscopic evidence for three actomyosin:ADP states in smooth muscle. *J. Biol. Chem.* **275**, 25418–25426.
43. Wang, F., Kovacs, M., Hu, A., Limouze, J., Harvey, E. V. & Sellers, J. R. (2003). Kinetic mechanism of non-muscle myosin IIB: functional adaptations for tension generation and maintenance. *J. Biol. Chem.* **278**, 27439–27448.

Please cite this article as: Purcell, T. J. *et al.*, Nucleotide Pocket Thermodynamics Measured by EPR Reveal How Energy Partitioning Relates Myosin Speed to Efficiency, *J. Mol. Biol.* (2011), doi:10.1016/j.jmb.2010.11.053

44. De La Cruz, E. M., Wells, A. L., Rosenfeld, S. S., Ostap, E. M. & Sweeney, H. L. (1999). The kinetic mechanism of myosin V. *Proc. Natl Acad. Sci. USA*, **96**, 13726–13731.
45. Cremo, C. R. & Geeves, M. A. (1998). Interaction of actin and ADP with the head domain of smooth muscle myosin: implications for strain-dependent ADP release in smooth muscle. *Biochemistry*, **37**, 1969–1978.
46. Ritchie, M. D., Geeves, M. A., Woodward, S. K. & Manstein, D. J. (1993). Kinetic characterization of a cytoplasmic myosin motor domain expressed in *Dictyostelium discoideum*. *Proc. Natl Acad. Sci. USA*, **90**, 8619–8623.
47. Iorga, B., Adamek, N. & Geeves, M. A. (2007). The slow skeletal muscle isoform of myosin shows kinetic features common to smooth and non-muscle myosins. *J. Biol. Chem.* **282**, 3559–3570.
48. Miller, B. M., Nyitrai, M., Bernstein, S. I. & Geeves, M. A. (2003). Kinetic analysis of *Drosophila* muscle myosin isoforms suggests a novel mode of mechanochemical coupling. *J. Biol. Chem.* **278**, 50293–50300.
49. Kurzawa, S. E. & Geeves, M. A. (1996). A novel stopped-flow method for measuring the affinity of actin for myosin head fragments using microgram quantities of protein. *J. Muscle Res. Cell Motil.* **17**, 669–676.
50. Highsmith, S. (1977). The effects of temperature and salts on myosin subfragment-1 and F-actin association. *Arch. Biochem. Biophys.* **180**, 404–408.
51. Woledge, R. C. (1968). The energetics of tortoise muscle. *J. Physiol.* **197**, 685–707.
52. Smith, N. P., Barclay, C. J. & Loiselle, D. S. (2005). The efficiency of muscle contraction. *Prog. Biophys. Mol. Biol.* **88**, 1–58.
53. Rall, J. A. & Schottelius, B. A. (1973). Energetics of contraction in phasic and tonic skeletal muscles of the chicken. *J. Gen. Physiol.* **62**, 303–323.
54. Clemen, A. E., Vilfan, M., Jaud, J., Zhang, J., Barmann, M. & Rief, M. (2005). Force-dependent stepping kinetics of myosin-V. *Biophys. J.* **88**, 4402–4410.
55. Lehmann, F. O. & Heymann, N. (2006). Dynamics of *in vivo* power output and efficiency of *Nasonia* asynchronous flight muscle. *J. Biotechnol.* **124**, 93–107.
56. Higashi-Fujime, S., Ishikawa, R., Iwasawa, H., Kagami, O., Kurimoto, E., Kohama, K. & Hozumi, T. (1995). The fastest actin-based motor protein from the green algae, *Chara*, and its distinct mode of interaction with actin. *FEBS Lett.* **375**, 151–154.
57. Pate, E. & Cooke, R. (1989). A model of crossbridge action: the effects of ATP, ADP and P_i. *J. Muscle Res. Cell Motil.* **10**, 181–196.
58. Karatzaferi, C., Chinn, M. K. & Cooke, R. (2004). The force exerted by a muscle cross-bridge depends directly on the strength of the actomyosin bond. *Biophys. J.* **87**, 2532–2544.
59. Spudich, J. A. & Watt, S. (1971). The regulation of rabbit skeletal muscle contraction. I. Biochemical studies of the interaction of the tropomyosin–troponin complex with actin and the proteolytic fragments of myosin. *J. Biol. Chem.* **246**, 4866–4871.
60. Malnasi-Csizmadia, A., Woolley, R. J. & Bagshaw, C. R. (2000). Resolution of conformational states of *Dictyostelium* myosin II motor domain using tryptophan (W501) mutants: implications for the open–closed transition identified by crystallography. *Biochemistry*, **39**, 16135–16146.
61. Tonomura, Y., Appel, P. & Morales, M. (1966). On the molecular weight of myosin. II. *Biochemistry*, **5**, 515–521.
62. Ikebe, M. & Hartshorne, D. J. (1985). Effects of Ca^{2+} on the conformation and enzymatic activity of smooth muscle myosin. *J. Biol. Chem.* **260**, 13146–13153.
63. Sweeney, H. L., Rosenfeld, S. S., Brown, F., Faust, L., Smith, J., Xing, J. *et al.* (1998). Kinetic tuning of myosin via a flexible loop adjacent to the nucleotide binding pocket. *J. Biol. Chem.* **273**, 6262–6270.
64. Weeds, A. G. & Taylor, R. S. (1975). Separation of subfragment-1 isoenzymes from rabbit skeletal muscle myosin. *Nature*, **257**, 54–56.
65. Yang, C., Ramanath, S., Kronert, W. A., Bernstein, S. I., Maughan, D. W. & Swank, D. M. (2008). Alternative versions of the myosin relay domain differentially respond to load to influence *Drosophila* muscle kinetics. *Biophys. J.* **95**, 5228–5237.

Please cite this article as: Purcell, T. J. *et al.*, Nucleotide Pocket Thermodynamics Measured by EPR Reveal How Energy Partitioning Relates Myosin Speed to Efficiency, *J. Mol. Biol.* (2011), doi:10.1016/j.jmb.2010.11.053